Geol. Mag. **147** (*5*), *2010, pp. 652–664.* © *Cambridge University Press 2010*
doi:10.1017/S0016756810000105

Mesoscopic and magnetic fabrics in arcuate igneous bodies: an example from the Mandi-Karsog pluton, Himachal Lesser Himalaya

R. JAYANGONDAPERUMAL, A. K. DUBEY & K. SEN*

Wadia Institute of Himalayan Geology, 33 GMS Road, Dehradun-248001, India

(*Received* 3 September 2009; *accepted* 9 December 2009; First published online 23 February 2010)

Abstract – Field, microstructural and anisotropy of magnetic susceptibility (AMS) data from the Palaeozoic Mandi-Karsog pluton in the Lesser Himalayan region reveal a concordant relationship between fabric of the Proterozoic host rock and the granite. The pluton displays a prominent arcuate shape on the geological map. The margin-parallel mesoscopic and magnetic fabrics of the granite and warping of the host rock fabric around the pluton indicate that this regional curvature is either synchronous or pre-dates the emplacement of the granite body. Mesoscopic fabric, magnetic fabric and microstructures indicate that the northern part of the pluton preserves its pre-Himalayan magmatic fabric while the central and southern part shows tectonic fabric related to the Tertiary Himalayan orogeny. The presence of NW–SE-trending aplitic veins within the granite indicates a post-emplacement stretching in the NE–SW direction. Shear-sense indicators in the mylonites along the margin of the pluton suggest top-to-the-SW shearing related to the Himalayan orogeny. Based on these observations, it is envisaged that the extension that gave rise to this rift-related magmatism had a NE–SW trend, that is, normal to the trend of the aplite veins. Subsequently, during the Himalayan orogeny, compression occurred along this same NE–SW orientation. These findings imply that the regional curvature present in the Himachal Lesser Himalaya is in fact a pre-Himalayan feature and the pluton has formed by filling a major pre-Himalayan arcuate extension fracture.

Keywords: Himalaya, Mandi-Karsog Pluton, granite, anisotropy of magnetic susceptibility, deformation, mylonites.

1. Introduction

Granite magmatism is often associated with transtensional and extensional tectonics (Hutton *et al.* 1990; Hutton & Reavy, 1992; Bouillin *et al.* 1993; Aranguren *et al.* 1996). Any inferences on the tectonic setting of granites depend heavily on detailed analysis of their internal fabric and that of the host rock. Deciphering tectonic events and mechanisms that give rise to pluton emplacement deals with: (1) the relationship between deformation in the country rock and emplacement of the granite; (2) comparison between fabric of the country rock and that of the granite; (3) study of fabric present within the granite to determine the conditions of fabric formation, infer rheological behaviour of the crystallizing magma, and investigate if there is any systematic strain distribution pattern within the pluton. Hence, detailed quantification of fabric within granite and its host rock is important to understand the exact nature of deformation in the country rock that triggered or accompanied the ascent, emplacement and consolidation of the granitic magma. However, quantification of fabric in granite can be a difficult task. For this purpose, anisotropy of magnetic susceptibility (AMS) is used extensively (Tarling & Hrouda, 1993; Bouchez, 1997). This, along with mesoscopic and microscopic studies, can provide valuable insights into the emplacement and subsequent tectonic evolution of a granitic pluton.

In the Himalayan region, emplacement of numerous granitic bodies between 450 and 600 Ma (Pan-African) involved both explosive volcanism and syntectonic intrusion (Valdiya, 1993, 1995). Islam *et al.* (1999) have carried out a detailed geochemical study of some of these Himalayan granites and inferred them to be peraluminous, S-type granites derived from a crustal source and related to the Pan-African rift magmatism. However, structural aspects of these granites have never been analysed. One such body, the Mandi-Karsog pluton, presents a prominent arcuate shape on the geological map (Fig. 1). The present study is an attempt to understand the nature of arcuation (pre-Himalayan or syn-Himalayan) and tectonic setting of this pluton with the help of field, microstructural and AMS analysis.

2. Geology of the area

The regional geology of the Himachal Lesser Himalaya (western Himalaya) has been described by Pilgrim & West (1928), LeFort (1975), Chatterji & Swaminath (1977), Srikantia & Bhargava (1998) and Dubey, Bhakuni & Selokar (2004) (Fig. 1). The Mandi-Karsog pluton lies within the Chail Formation and covers an area of ~ 30 km^2. The regional trend of the pluton is parallel to curvature of the adjacent Chail Thrust (that

*Author for correspondence: koushik.geol@gmail.com

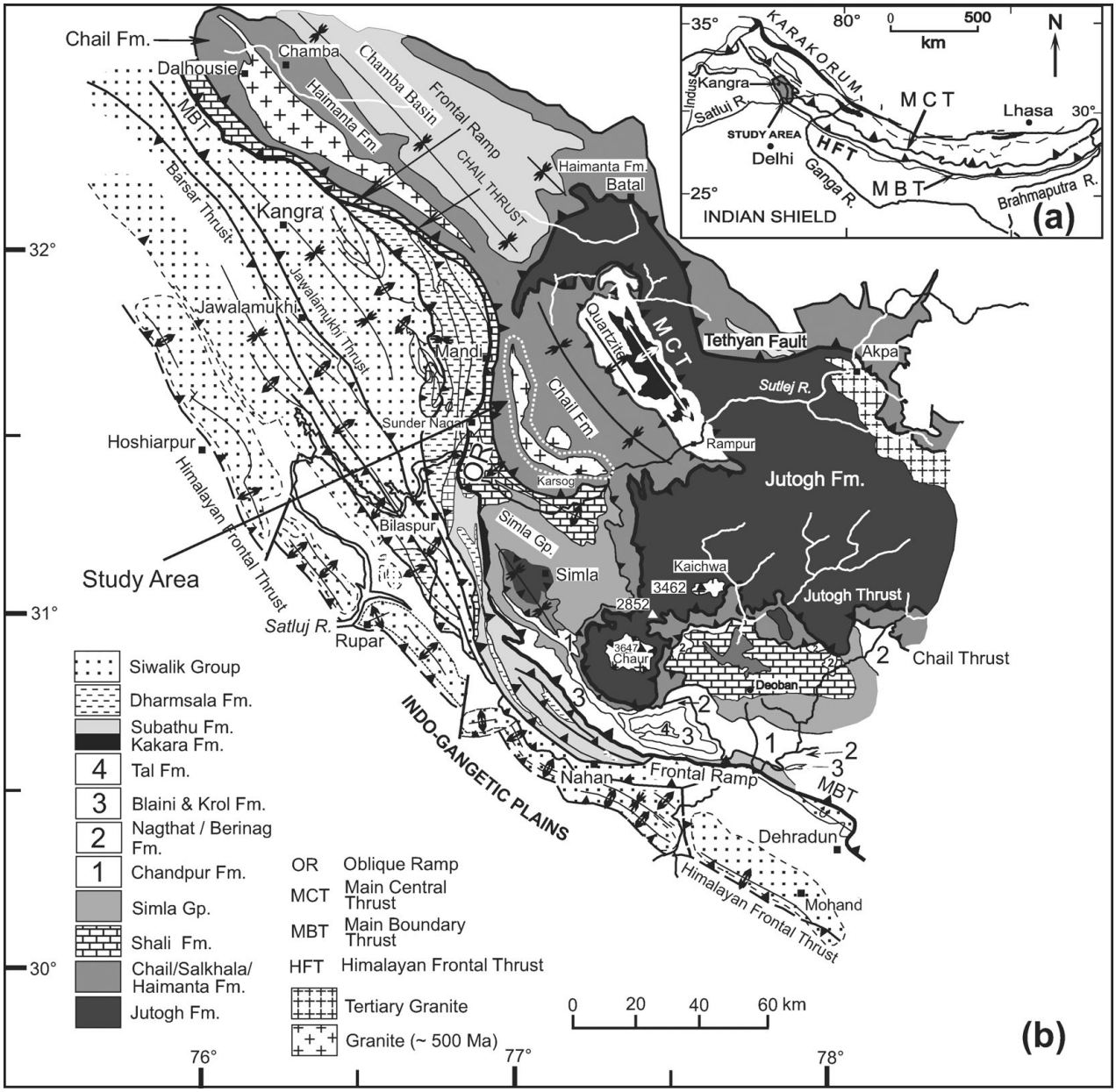

Figure 1. (a) Tectonic framework of the Himalaya. (b) Map showing regional geology of the Himachal Himalaya (after Thakur & Rawat, 1992; Srikantia & Bhargava, 1998). Irregular white polygon shows the study area.

is, N–S in the northern part, E–W in the southern part). The age of the pluton is poorly constrained by Rb–Sr dating to around 507 ± 100 Ma (Jäger, Bhandari & Bhanot, 1971). Miller *et al.* (2001) have carried out geochemistry and geochronology of the Kaplas pluton (north of the Mandi-Karsog pluton) and tholeiitic mafic rocks in the Mandi-Karsog area. The study provides evidence of magma mingling and close association of granitic and mafic magma in the Mandi-Karsog area. It was also ascertained that the mafic magma has a mantle source which crystallized at 496 ± 14 Ma, whereas the granitic part was derived from a crustal source and crystallized at 553 ± 2 Ma. Based on these data, an asthenospheric upwelling and passive crustal extension model was favoured for generation of the pluton. This conclusion is in support of the earlier rift tectonics model (Bhat, Zainuddin & Rais, 1981). The model considers that the prominent Himalayan thrusts were formed as normal faults during the pre-Himalayan tensional regime in the region and reactivated as thrusts during the Tertiary Himalayan orogeny (Bhat, 1987; Dubey, Bhakuni & Selokar, 2004). These studies suggested that fissures generated during the Pan-African rifting assisted the ascent and emplacement of the granitic magma.

3. Field observations

3.a. Structures in the host rock

The pluton intrudes quartzites, schists and calc-silicate rocks of the Proterozoic Chail Formation. The host rock exhibits a margin-parallel foliation with the pluton with low to moderate dip towards the E or NE (Fig. 2a),

https://doi.org/10.1017/S0016756810000105 Published online by Cambridge University Press

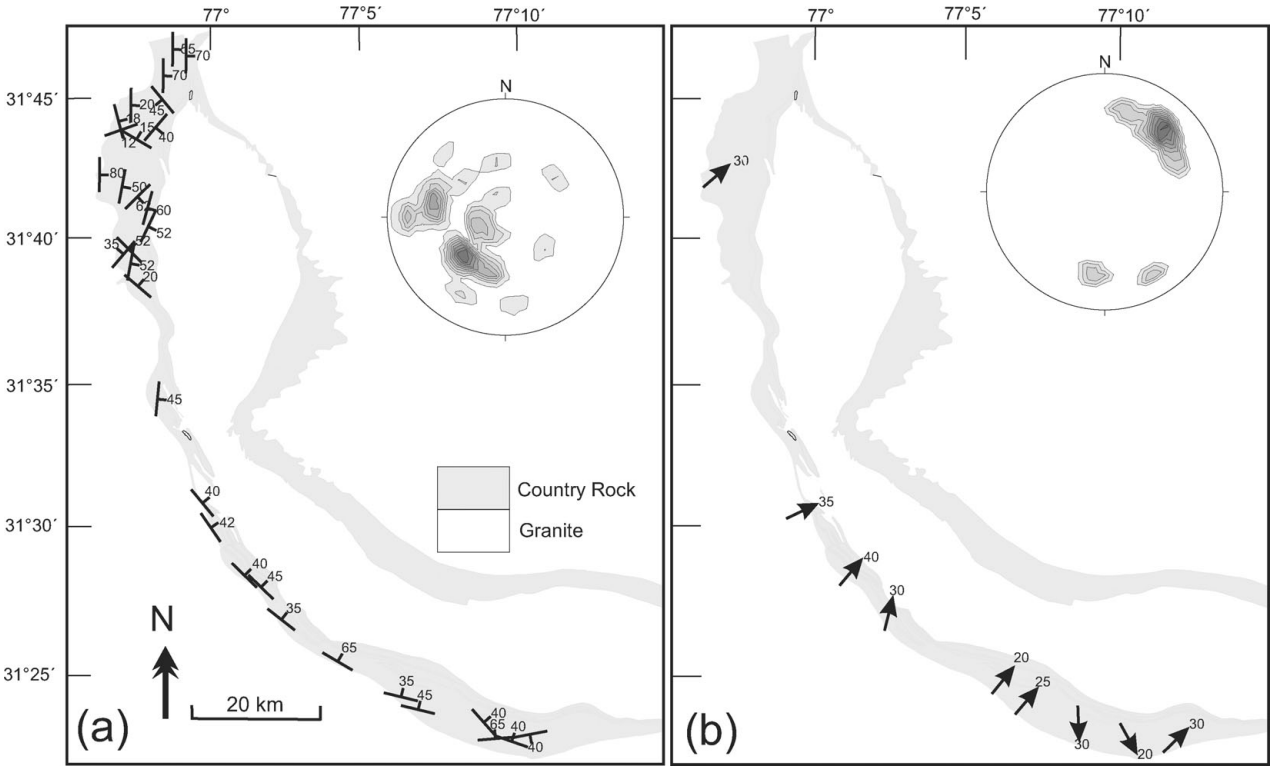

Figure 2. (a) Foliation in the host rock of the Mandi-Karsog pluton with density contour in lower hemisphere equal area projection of poles. (b) Lineation present in the host rock with density contour in lower hemisphere equal area projection.

except in areas of superimposed folding. The stretching mineral lineation shows a moderate plunge towards the NE (Fig. 2b) (Steck, 2003; Dubey, Bhakuni & Selokar, 2004). Variation in the direction of plunge can be observed as a result of non-cylindrical folding.

3.b. Structures in the Mandi-Karsog Pluton

The pluton is generally muscovite and biotite bearing coarse and porphyritic granite that has later been intruded by injections of aplitic veins in places. In the core of the pluton, the feldspar laths show random orientations. However, in other parts they define a well-developed foliation that is concordant with the margin and generally NNE dipping (Fig. 3a) (see also Thakur, 1975). The western margin of the pluton, which has been studied in detail, is characterized by presence of mylonites in its central and southern parts that show stretching lineation having a dominantly NE plunge to a moderate extent (Fig. 3b). The western margin of the pluton has been intruded by a band of tourmaline granite striking N–S. The tourmaline crystals show mostly NW–SE to N–S trends. The aplitic veins have a NW–SE strike. The field relationship suggests that the aplitic veins and the tourmaline-bearing granites are younger than the coarse-grained and porphyritic varieties of the two-mica granites. The mesoscopic features show the presence of a primary magmatic fabric defined by preferred orientation of euhedral to subhedral feldspar laths in the northern part of the pluton (Fig. 4a) and a tectonic fabric defined by deformed granitic gneiss with feldspar porphyroclasts in the southern part (Fig. 4b). Contact between the granite and the Chail rock is parallel to foliation in the host rock (Fig. 4c). In some places, the granite shows interfingering with quartzite and schist of the Chail Formation (Fig. 4d).

4. AMS measurement

4.a. Sampling and methodology

The anisotropy of magnetic susceptibility (AMS) was measured by a KLY-3S Kappabridge (Agico, Czech Republic) in the Paleomagnetic Laboratory of the Wadia Institute of Himalayan Geology. Oriented block samples were taken from 24 sites within the pluton (Fig. 5). These block samples were drilled in the laboratory and 158 core specimens were obtained for analyses. For measurement of various parameters, the number of core specimens per site varied from six to eight. Depending on location of the site along the curvature, the entire Mandi-Karsog pluton was divided into three parts: northern sector (sector A), central sector (sector B) and southern sector (sector C). The database (Table 1) provides the orientation and magnitude of the three principal axes of the magnetic susceptibility ellipsoid ($K1 \geq K2 \geq K3$). The magnetic lineation is parallel to K1 and pole to the magnetic foliation (K1–K2 plane) is parallel to K3. The magnitudes of these principal directions were used to calculate different parameters such as; K_m (mean magnetic susceptibility), P′ (corrected degree of magnetic anisotropy), which is a measure of

https://doi.org/10.1017/S0016756810000105 Published online by Cambridge University Press

Table 1. AMS data from the samples from the Mandi-Karsog pluton

Location	n	K_m (μSI)	L	F	P′	T	K1	K3	Sector
PM3	10	55.5	1.033	1.069	1.107	0.343	325/20	83/52	A
PM4	6	55.3	1.033	1.056	1.092	0.243	15/18	244/62	A
PM6	7	239	1.034	1.035	1.071	0.018	355/13	175/76	A
PM8	6	57.5	1.031	1.083	1.12	0.447	169/14	325/74	A
PM9	6	118	1.024	1.126	1.166	0.655	340/3	253/67	A
DC2	4	8.66	1.014	1.051	1.071	0.542	73/41	273/45	A
PG7	10	29.9	1.063	1.153	1.233	0.39	30/24	130/20	B
CB2	3	85.5	1.018	1.018	1.038	–0.006	30/29	275/38	B
BC1	2	65.5	1.032	1.093	1.136	0.4935	109/56	262/27	B
BC2	10	47.9	1.018	1.088	1.116	0.652	25/20	270/38	B
CK1	10	257	1.024	1.04	1.067	0.261	74/24	189/44	B
SK9	5	33.6	1.021	1.105	1.139	0.659	65/18	178/51	C
SK11	20	279	1.028	1.067	1.1	0.396	69/9	155/67	C
SK13	4	53	1.023	1.161	1.206	0.728	353/39	177/51	C
SK14	1	295	1.015	1.152	1.189	0.808	44/36	168/38	C
KK1	10	217	1.027	1.038	1.067	0.146	79/47	237/40	C
KK2	10	204	1.015	1.032	1.05	0.342	252/75	16/6	C
KK3	9	227	1.012	1.045	1.062	0.573	110/20	16/31	C
KK5	9	198	1.013	1.051	1.069	0.548	103/21	208/32	C
KK7	3	70.6	1.022	1.081	1.111	0.554	354/62	179/27	C
KL2	6	113	1.019	1.121	1.155	0.718	82/26	198/46	C
KL3	10	96.8	1.01	1.023	1.034	0.384	259/19	158/34	C
KL5	3	154	1.011	1.126	1.155	0.832	265/9	193/61	C
KL7	4	99.1	1.038	1.17	1.23	0.61	49/4	143/67	C

n = No. of specimen; K_m – magnitude of susceptibility (in 10^{-6} SI); L – magnetic lineation ((K1–K2)/K_m); F –magnetic foliation ((K2– K3)/K_m); P′ – corrected degree of magnetic anisotropy (Jelinek, 1981); T – shape parameter (Jelinek, 1981); K1 – declination and inclination (in degrees) of magnetic lineation; K3 – declination and inclination (in degrees) of normal to magnetic foliation plane.

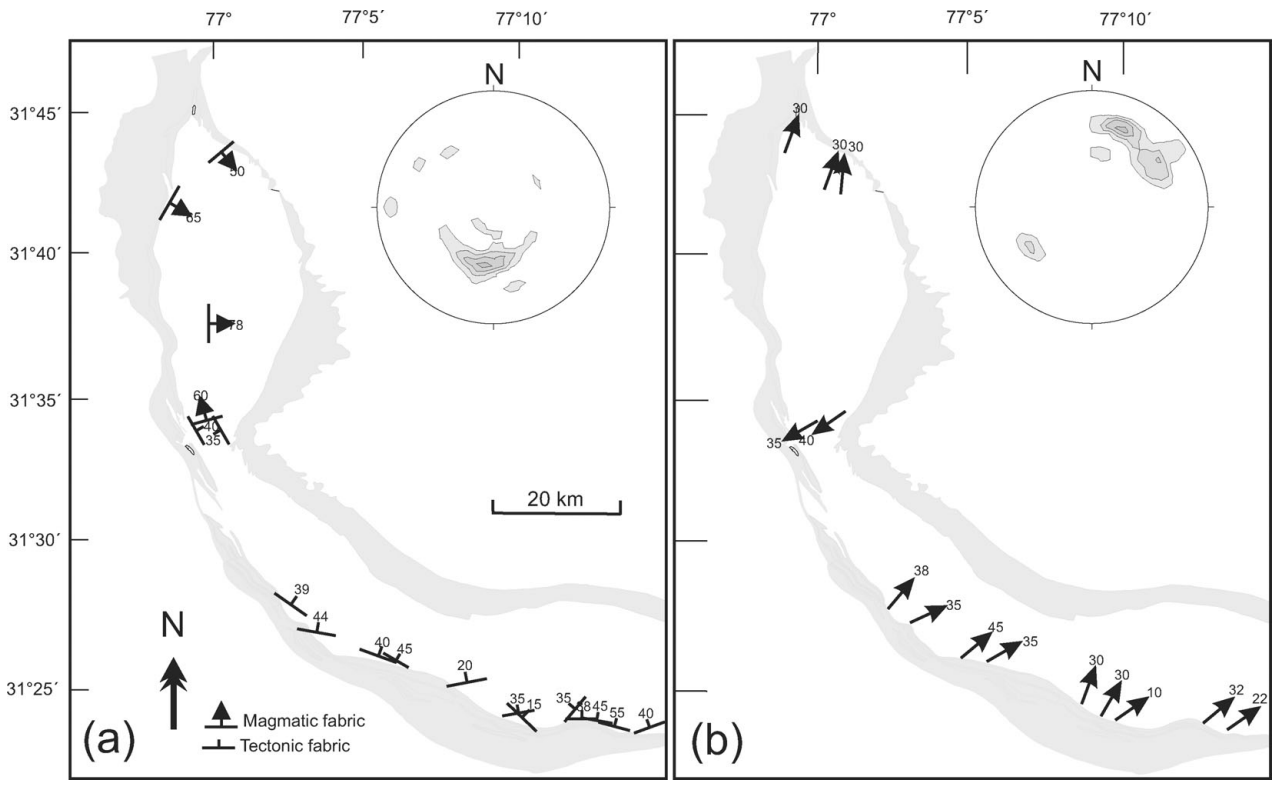

Figure 3. (a) Foliation in the Mandi-Karsog pluton. Inset shows lower hemisphere density stereogram of pole to mesoscopic foliation. (b) Lineation present in the Mandi-Karsog pluton. Inset shows lower hemisphere density stereogram of mesoscopic lineation.

eccentricity of the magnetic susceptibility ellipsoid (Jelinek, 1981), L (magnetic lineation), F (magnetic foliation) and T (shape parameter that describes the oblate/prolate shape of the magnetic susceptibility ellipsoid; Tarling & Hrouda, 1993). The software SUSAR attached to the KLY-3S Kappabridge was used to calculate the above parameters. The average orientation for magnetic lineation (K1) and pole to the magnetic foliation (K3) were computed for each site. When the confidence level of a magnetic axis is lower

https://doi.org/10.1017/S0016756810000105 Published online by Cambridge University Press

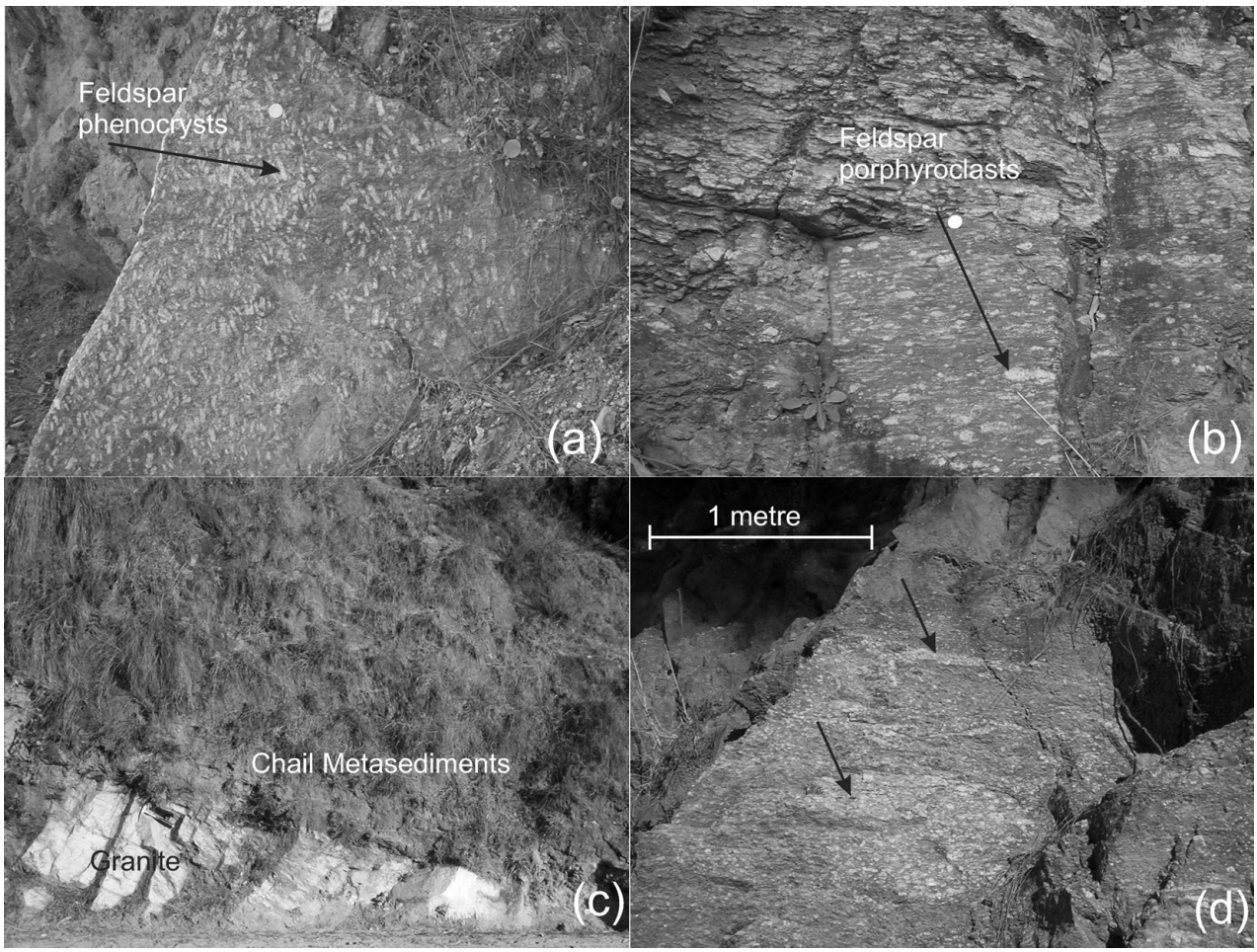

Figure 4. Mesoscopic features in the Mandi-Karsog pluton. (a) Oriented laths of feldspar phenocrysts showing magmatic fabric. Coin for scale. (b) Mylonite with feldspar porphyroclasts. Coin for scale. (c) Foliation-parallel contact between the granite and the host Chail rock. Hammer for scale. (d) Interfingering of granitic material (black arrows) within the host Chail rocks.

than 20° within a site, the axis is considered to be well defined (see Table 1 for complete AMS data).

4.b. Parameters of magnetic anisotropy

Granites with $K_m > 500$ μSI are considered to be ferromagnetic, while those with $K_m < 500$ μSI are classified as paramagnetic (Bouchez, 1997). While paramagnetic minerals such as biotite and hornblende comprise paramagnetic granites, ferromagnetic (*s.l.*) minerals like magnetite are responsible for high K_m values in ferromagnetic granites. The AMS data reveal that the Mandi-Karsog pluton is paramagnetic with K_m values between 8.66 μSI (DC2) and 279 μSI (SK11) (Table 1). The frequency histogram of K_m shows that all of the 158 specimens have K_m values less than 300 μSI (Fig. 6a). The lowest P′ value is 1.034 (KL3), whereas the highest P′ value is 1.233 (PG7). Most of the samples in the pluton have P′ values between 1 and 1.15. In the northern part (sector A), all the specimens have P′ values < 1.2, while some specimens from sectors B and C have values > 1.25. For all three sectors of the Mandi-Karsog pluton, there is no one-to-one correlation between P′ and K_m, indicating that the AMS fabric is not governed by magnetic mineralogy (Rochette, 1987; Borradaile & Henry, 1997) (Fig. 6b). It may also be noted that only one site each from the northern and central sectors has P′ value > 1.15, whereas sites with higher P′ values are mostly from the southern sector (sector C). The shape parameter (T) indicates a strong oblate fabric for most of the sites with T values > 0.24 for all but three sites (Table 1). This indicates a strong flattening fabric in the entire pluton. One site each from the northern and central sectors shows plain strain or a triaxial susceptibility ellipsoid (Fig. 6c). The magnetic foliation (F) has a linear relationship with P′ for all the sites (Fig. 6d). The magnetic lineation (L) shows a weak linear relationship with P′ for sectors B and C. No such relation was found in sector A (Fig. 6d). This suggests a control of deformation on the development of magnetic foliation and lineation.

4.c. Magnetic fabric

The magnetic foliation in the pluton is dominantly margin-parallel. The dip of the magnetic foliation is moderate and dominantly towards the north or east,

https://doi.org/10.1017/S0016756810000105 Published online by Cambridge University Press

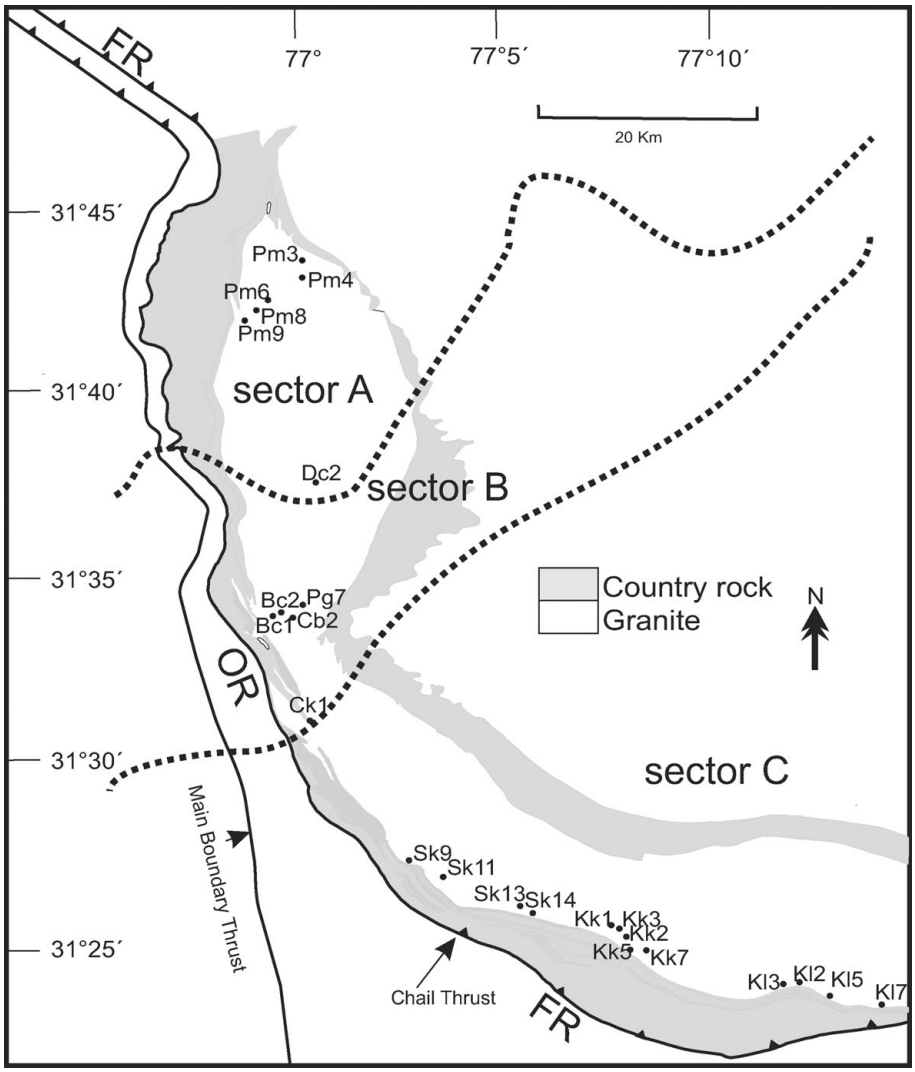

Figure 5. Map showing location of samples for AMS along with the associated Chail thrust and Main Boundary Thrust (MBT). Dotted lines are arbitrary dividers between the three sectors. Frontal (FR) and oblique (OR) fault ramps.

depending on the trend of the pluton margin (Fig. 7). In general, the foliation has much steeper dips in the central and southern sectors than the northern one. The magnetic lineation in sector A has a N–S trend with a gentle plunge (average 6°). In the central part (sector B), they are dominantly NW-plunging. In the southern part (sector C), the magnetic lineation trend varies from NW to almost E–W (Fig. 7). The average plunge is 24° for sectors B and C.

5. Microstructures

5.a. The granite

The Mandi-Karsog pluton is essentially made up of quartz, feldspar, muscovite, and biotite. Samples in the northern sector (PM-3, PM-4, PM-6, etc.) preserve primary magmatic features like oscillatory zoning in plagioclase (Fig. 8a), euhedral feldspar grains and subsolidus cooling structures like exsolution lamellae in K-feldspar (Fig. 8b). In contrast, the central and southern sectors show features like warping of muscovite around feldspar porphyroclasts (Fig. 8c) and kinking in muscovite (Fig. 8d). Plagioclase grains showing bent twins and 'core and mantle' structures in feldspar porphyroclasts are also seen. All these features suggest that the central and southern sectors have suffered medium- to low-temperature solid state deformation related to the Tertiary Himalayan orogeny.

5.b. Mylonites and the host rock

To understand the nature of deformation that affected the granite, the mylonites present along the pluton rim in the western margin of the central and southern sectors were studied. Features like 'delta'-type porphyroclasts (Fig. 8e) and imbrication of feldspar laths (Fig. 8f) were seen. In general, the mylonite microstructures indicate 'top-to-the-SW' shearing related to the Himalayan orogeny. The host rocks show evidence of brittle deformation under the microscope (Fig. 8g). Evidence of brittle deformation was also seen in quartz veins within the host rock (Fig. 8h), indicating a later deformation event.

https://doi.org/10.1017/S0016756810000105 Published online by Cambridge University Press

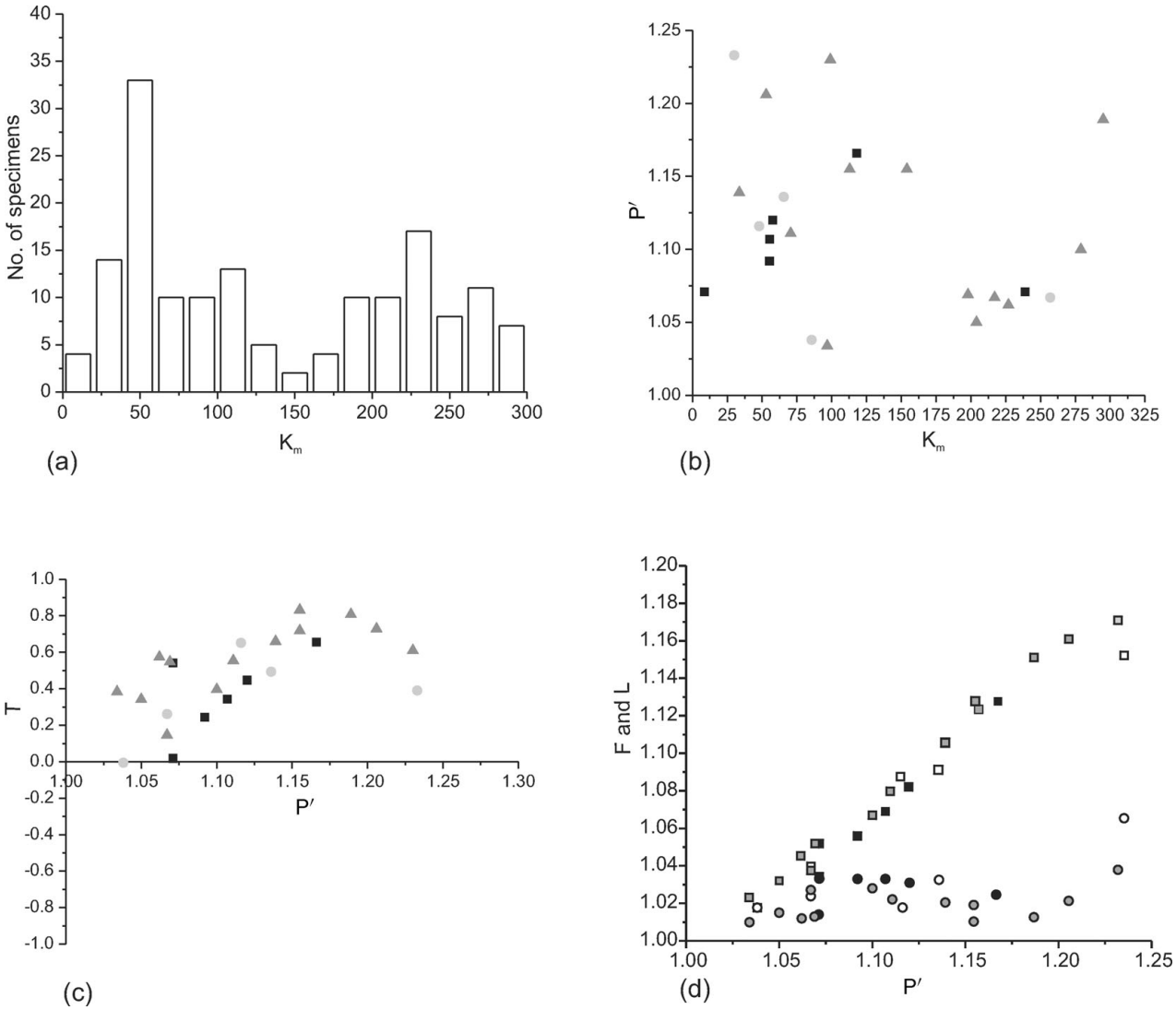

Figure 6. (a) Frequency histogram showing distribution of Mean Magnetic Susceptibility (K_m) for all the specimens. (b) Graph showing relation between K_m and P′ for all the samples. Black square – northern sector; light grey circle – central sector; grey triangle – southern sector. (c) Jelinek plot showing relation between P′ and T. Legend as in (b). (d) Graph showing relation between P′ and F (squares) and between P′ and L (circles). Legend: black square – northern sector; white square – central sector; grey square – southern sector; black circle – northern sector; white circle – central sector; grey circle – southern sector. L – magnetic lineation; F – magnetic foliation.

6. Discussion

6.a. Deformation and pluton growth

The relationship between the host rock fabric and fractures that caused ascent of granitic melt is important for understanding the dynamics of syn-emplacement growth of a pluton (Castro & Fernandez, 1998). For concordant plutons, that is, where the host rock fabric and the pluton fabric remain margin-parallel, the deflection of the host rock fabric can be a useful indicator to aid in understanding the syn-emplacement dynamics. In the Mandi-Karsog area, the host rock has a more or less NNW–SSE-trending fabric. The southern part of the pluton is parallel to this fabric but its trend is oblique in the northern part. The host rock fabric deflects a few kilometres north of the northern tip of the pluton. The margin-parallel fabric, along with deflection of the foliation trajectories around the pluton, suggests a partial coupling between the host rock and the granite (cf. Paterson *et al.* 1998). It indicates that, along with fracture propagation, the granitic melt has grown laterally by forcing its way into the country rock while deforming the margin. The deflection of host rock fabric due to emplacement and growth of a pluton has been described by many workers (e.g. Corry, 1988; Geoffrey, Olivier & Rochette, 1997; O'Driscoll *et al.* 2006; Stevenson, Owens & Hutton, 2007). Petronis *et al.* (2009) have studied the Western granite of NW Scotland and shown that bedding in the host Torridonian varies significantly from its regional trend near its contact with the granite. They argued that the host rock fabric has been deflected and deformed due to emplacement and expansion of the pluton. Hence, in the present case, it can be argued that the deflection of foliation in the host rock was contemporaneous with emplacement of the Mandi-Karsog pluton.

https://doi.org/10.1017/S0016756810000105 Published online by Cambridge University Press

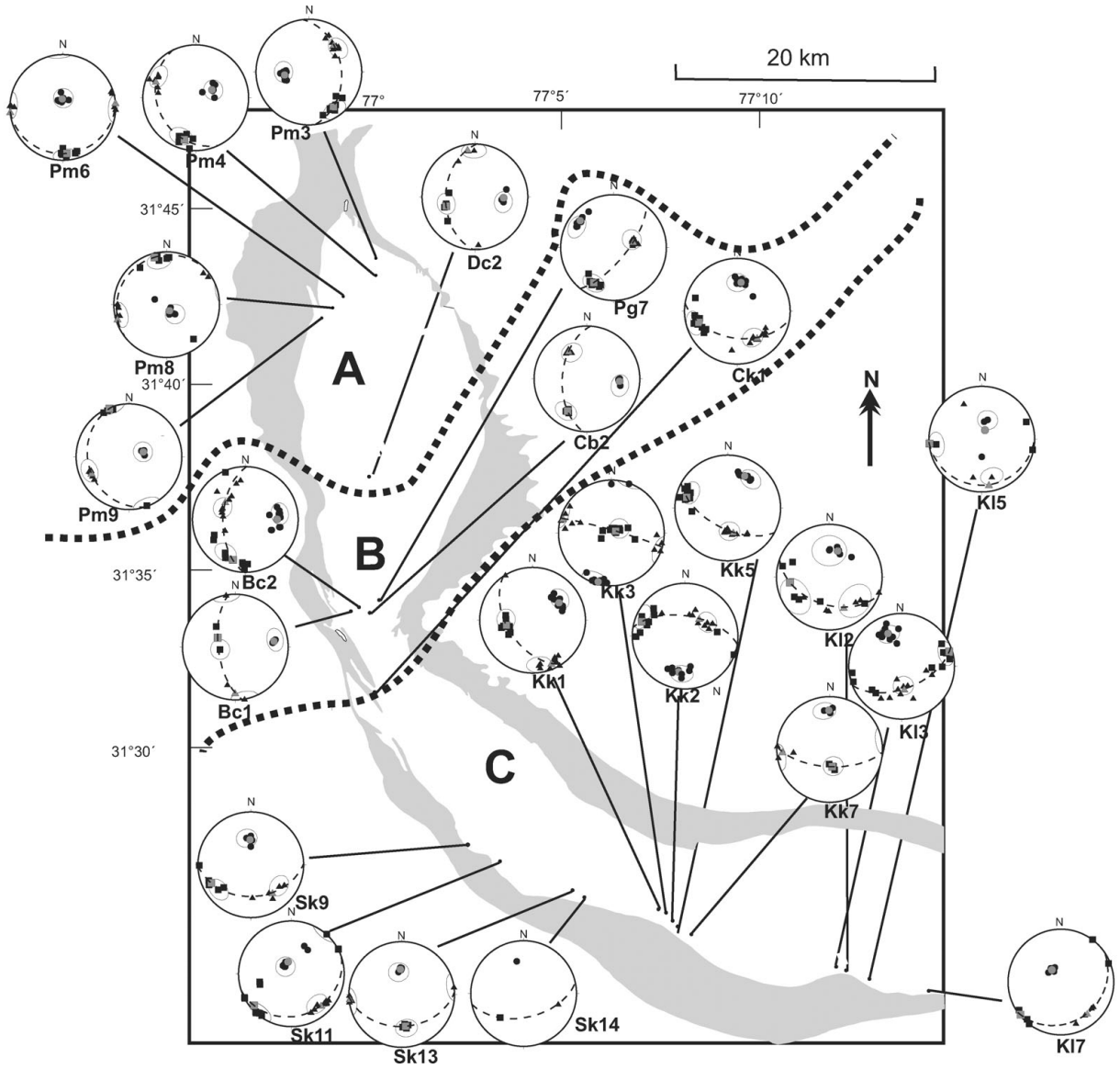

Figure 7. Pattern of magnetic foliation and lineation of all the sites within the Mandi-Karsog pluton with the help of lower hemisphere equal area projections of K1 (black square), (grey square – mean K1); K2 (black triangle), (grey triangle – mean K2); K3 (black circle), (grey circle – mean K3); dashed girdle shows the K1–K2 plane (magnetic foliation). (K3 – sector A: n = 6, maximum density at 255/66; sector B: n = 5, maximum density at 270/42; sector C: n = 13, maximum density at 189/48). (K1 – sector A: n = 6, maximum density at 343/6; sector B: n = 5, maximum density at 27/24; sector C: n = 12, maximum density at 104/24).

6.b. Post-emplacement stretching

The orientation of aplitic or pegmatite veins and tourmaline-bearing melt intruding a granitic pluton are useful indicators of the stretching direction of the pluton (Bouchez, 1997). As these are residual parts of the magma, they intrude after or at the final stage of emplacement. They occupy the fractures present within the pluton. In plutons related to regional shearing movement, fractures develop normal to the direction of maximum stretching. Within the Mandi-Karsog pluton, the aplitic veins that intruded the porphyritic and coarse-grained granite have a dominantly NW–SE trend. This, in turn, implies that the granitic body has undergone stretching in a NE–SW direction, which coincides with the pre-Himalayan extension direction (Bhat, 1987).

6.c. Effect of the Himalayan orogeny

On the basis of field and magnetic investigations it is unclear whether the orientation of granitic fabric has undergone any significant modification during the Himalayan orogeny. However, the effect of the Himalayan orogeny can be envisaged with the help of the following:

(1) the microstructures revealing intense solid state deformation and mylonitization in the southern and central sectors;

(2) steeper dips of the magnetic foliation in the central and southern sectors of the pluton which were likely caused by a late compressional phase;

(3) the greenschist–epidote–amphibolite-grade regional metamorphism in the Chail rocks during the Tertiary Himalayan orogeny (Gururajan & Virdi, 1984);

https://doi.org/10.1017/S0016756810000105 Published online by Cambridge University Press

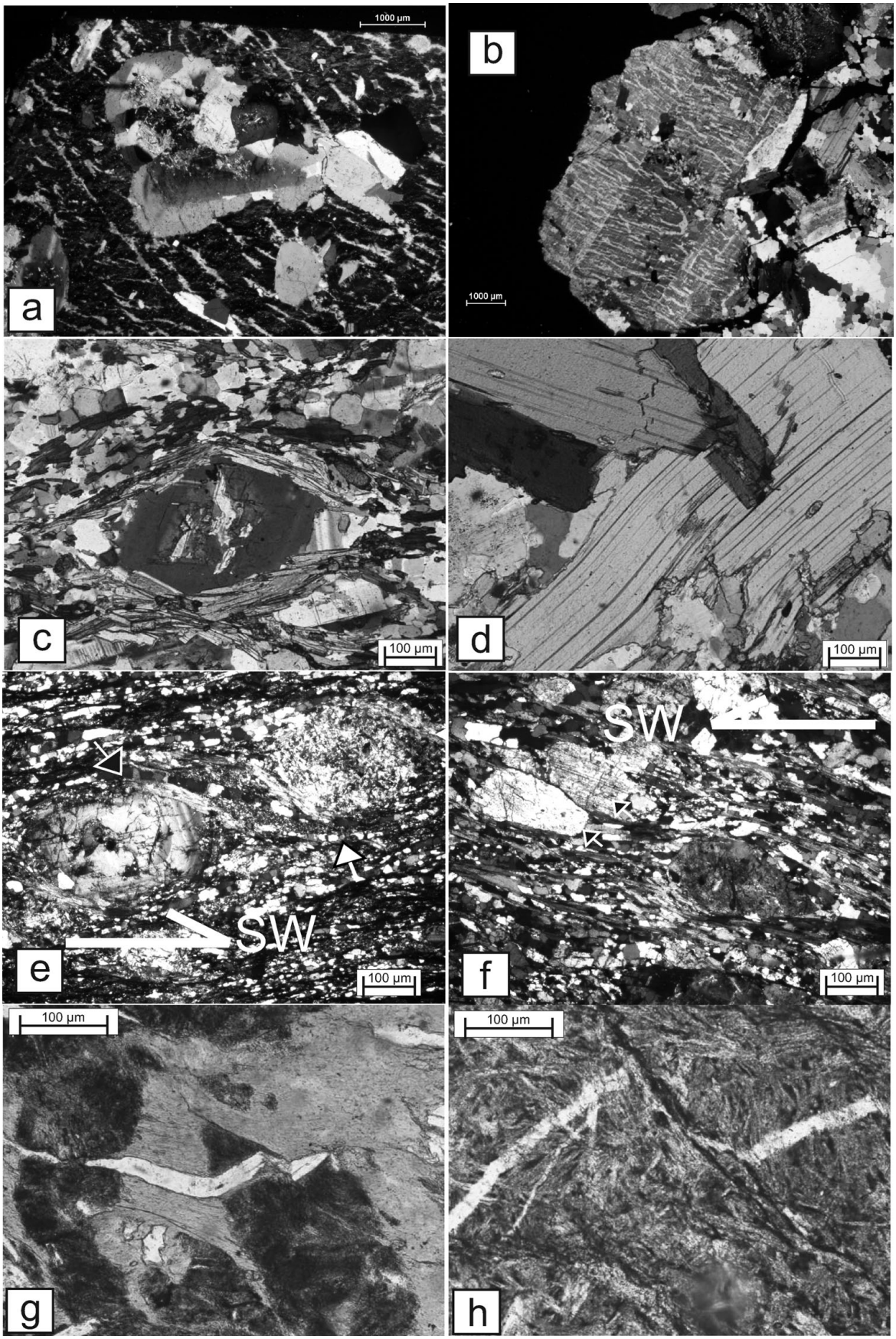

Figure 8. Microstructural features of the Mandi-Karsog pluton and its host rock. (a) Oscillatory zoning in plagioclase. (b) Exsolution texture in feldspar. (c) Warping of muscovite around plagioclase phenocryst. Note the igneous texture of the phenocryst. (d) Microkink in muscovite. (e) 'Delta'-type porphyroclast (black arrow) and its 'tail' (white arrow) showing dextral sense of shear (top-to-the-SW) (sample no. SK8). (f) Imbrication or 'tiling' of feldspar laths showing sinistral sense of shear (top-to-the-SW) (sample no. SK13). (g) Microfaulting in mica flakes of country rock (northern sector). (h) Faulting in quartz vein within the country rock.

https://doi.org/10.1017/S0016756810000105 Published online by Cambridge University Press

(4) the microstructural evidence of brittle deformation in the host rock and microfaulting in silicic veins by a later deformation event.

6.d. Tectonic evolution of the Mandi-Karsog Pluton in terms of magmatic and magnetic fabric

AMS study of a granite that has undergone a considerable amount of solid state deformation generally reveals a composite fabric, that is, where the field and magnetic fabrics become discordant (Aranguren, Cuevas & Tubia, 1996; Tomezzoli, McDonald & Tickyj, 2003). However, the Mandi-Karsog pluton shows an almost concordant relationship between the field and magnetic fabrics. In the northern sector it is expected, since this sector has not suffered much post-crystallization deformation during the Tertiary orogeny. Despite intense mylonitization, the central and southern sectors show almost similar strike in their mesoscopic and magnetic fabrics. It is envisaged that since the direction of pre-Himalayan extension and the direction of maximum compression related to Himalayan orogeny are similar, that is, a NE–SW direction, the strike of mesoscopic and magnetic foliations remained more or less parallel even in the central and southern sectors. Only the magnetic foliation became steeper during the Himalayan orogeny. Apart from this, almost all the locations in sector C dip towards the south, which is opposite to the dip of the adjacent Chail thrust. The steeper magnetic foliation depicting late stage compression is expected because this region was reactivated as a thrust during Tertiary times. We believe the discrepancy between dip direction of the thrust and that of the magnetic foliation is also caused by deformation during the Himalayan orogeny as AMS may represent fabric of thrust-related superposed folding in sector C.

The northern sector of the Mandi-Karsog pluton is almost free of mylonitization. Unlike the other two sectors, this part has been least effected by the Himalayan orogeny and preserves the emplacement-related fabric (Fig. 4a). The phenomenon is exemplified by the presence of magmatic to subsolidus microstructures (Fig. 8a, b) and substantiated by the relatively higher P′ values in the central and southern sectors (Fig. 6b–d). Since the P′ values in the pluton are not controlled by mean susceptibility (Fig. 6b), it can be argued that the higher degree of magnetic anisotropy in the southern part can only be caused by higher intensity of deformation (Sen & Mamtani, 2006). The stronger compressional fabric and its dependence on degree of anisotropy (P′) (Fig. 6c, d) in the central and southern sectors of the pluton also indicate a higher intensity of deformation in these areas. Since both the mesoscopic and magnetic fabrics in the northern sector show margin-parallel orientation, it can be inferred that their formation took place along a pre-existing curvature. This in turn suggests that the regional curvature of the Mandi-Karsog Pluton is a pre-Himalayan feature.

The tectonic evolution of the pluton appears to have occurred in the following stages (Fig. 9). The pre-Himalayan tensional regime in the Himalaya (predominant maximum extension in the NE–SW direction) led to initiation of fractures in the region. The heterogeneous nature of the crust was responsible for formation of irregular geometry and orientation of the fractures (Fig. 9a). These fractures propagated by extending their length and joined to form frontal and oblique fault ramps (Fig. 9b). The oblique fault ramp shows vertical and sinistral horizontal components of displacements. Ascent and emplacement of granitic melt may have taken place along the fractures. However, in the field, we found only a few occurrences of alternating screens of host rocks within the granite or sheeted nature in the granite that would suggest ascent and emplacement through fractures. Hence, it is suggested that ascent of the pluton took place by intruding sites of low stress near the curved normal fault, and subsequently it forced its way into the country rock by lateral expansion. The arcuate geometry of the fault resulted in the arcuate pattern of the granitic body. During the emplacement and expansion of the pluton, the initial host rock fabric deflected and warped around the pluton (Fig. 9c). Folding in the host rock suggests that expansion of the pluton was facilitated by ductile shortening of the host rock. Minor extensional fractures that are syn- to post-emplacement were filled up by late injections of aplitic veins. Finally, during the Tertiary compressional phase of the Himalayan orogeny, reactivation of the early normal fault took place as thrust. The initial sinistral displacement was also reactivated as right lateral displacement (Fig. 9d). Development of the mylonites may be attributed to displacement along the nearby thrust (Chail Thrust). These evolutionary stages reveal that the geometrical arcuation of the pluton is pre-Himalayan.

The primary nature of arcuation of the Main Boundary Thrust and Chail Thrust (Fig. 1) and their origin during the pre-Himalayan times are also apparent from the following facts.

(1) The Main Boundary Thrust, Shali thrust and Chail thrust show an arcuate pattern, whereas the Himalayan Frontal Thrust and other thrusts in the Siwalik rocks occurring in the Foothill Belt show a linear pattern.

(2) A pull-apart basin filled by Tertiary rocks is present at the Main Boundary Thrust (Dharamshala Formation, Fig. 1).

(3) The pre-Himalayan normal faulting is also indicated by early workers (Srikantia & Bhargava, 1979; Virdi, 1994) with evidence from the following:

(a) The various litho-units of the area show an eastward increase in thickness, indicating that the basin has deepened towards the east.

(b) In the area west of the Main Boundary Thrust, an oblique ramp remained exposed from the Late Proterozoic to Jurassic.

(c) An eastward palaeo-slope is indicated by palaeo-currents (Gaetani, Garzanti & Tintori, 1990).

https://doi.org/10.1017/S0016756810000105 Published online by Cambridge University Press

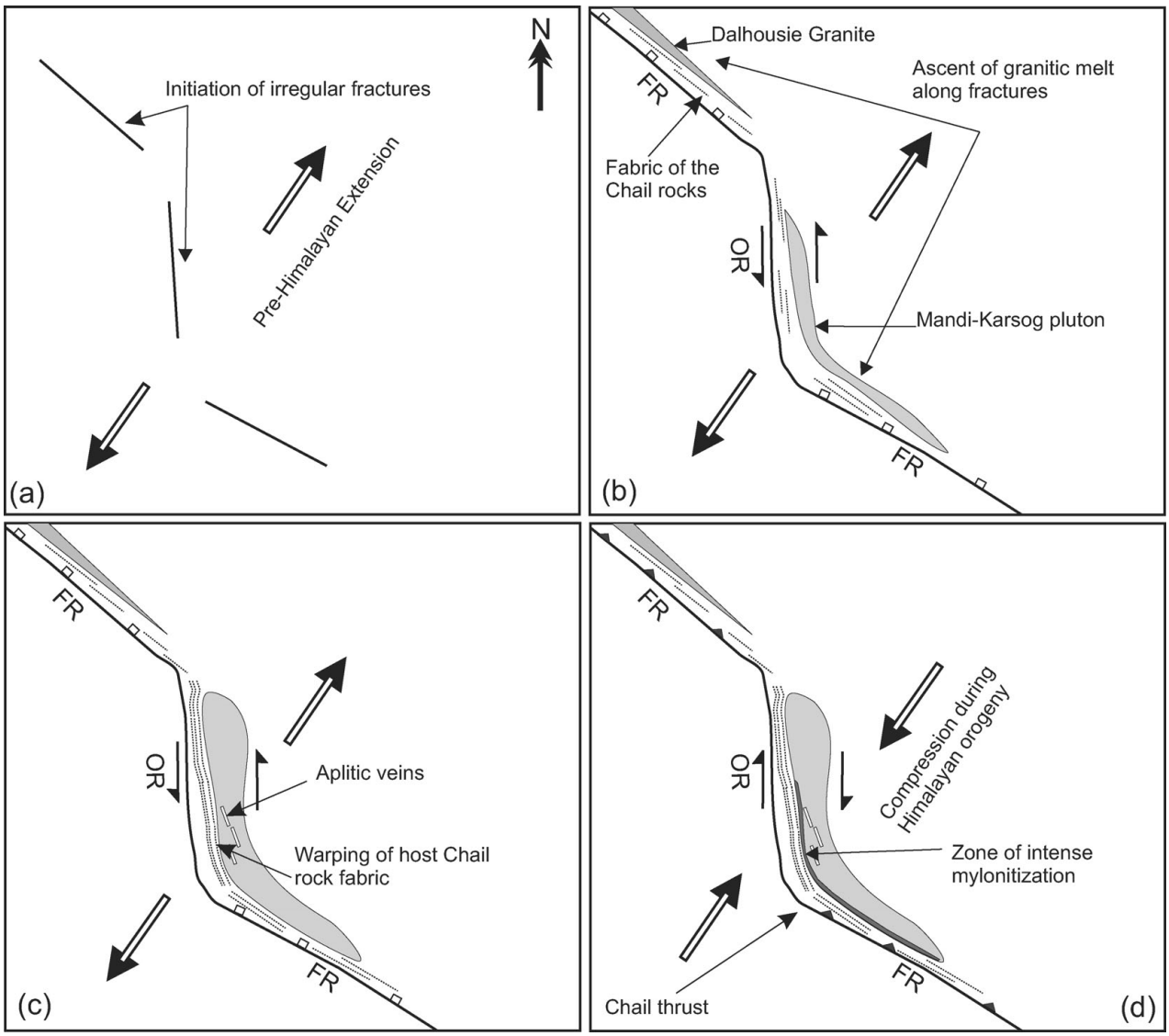

Figure 9. A simplified diagram showing structural evolution of the Mandi-Karsog pluton (not to scale). (a) Initiation of irregular fractures in heterogeneous Chail Formation during the pre-Himalayan tensional regime. The predominant stretching direction was NE–SW. (b) Propagation and linking of fractures as frontal (FR) and oblique (OR) normal fault ramps. The oblique ramp shows a component of sinistral strike-slip displacement. Ascent and emplacement of granitic melt along the fault. (c) Emplacement of the pluton results in the host rock fabric to deflect into parallelism with the intrusion. Minor extensional fractures were filled by aplitic veins. (d) Reactivation of the early normal fault as thrust during the Tertiary compressional phase of the Himalayan orogeny. Note the reversal of slip-sense along the OR fault. Mylonitization took place along the western margin of the pluton that is close to the Chail thrust.

7. Conclusions

By integrating the findings of the present study with those of Miller *et al.* (2001) and Dubey, Bhakuni & Selokar (2004) the following conclusions can be drawn.

(1) The pre-Himalayan oblique-slip extension direction was ~NE–SW, along which the granitic melt ascended during the Pan-African extensional tectonics.

(2) Arcuation of the Mandi-Karsog pluton is a primary feature.

(3) The syn-Himalayan compression direction was also NE–SW.

(4) Due to extension and subsequent compression along the same direction, the mesoscopic and magnetic fabrics of the Mandi-Karsog pluton have a concordant relationship.

(5) The intensity of deformation increases from the north to the south of the pluton. While the northern sector retained its primary magmatic fabric, the central and southern sectors suffered considerable solid state deformation during the Himalayan orogeny.

Acknowledgements. We are grateful to Michael Petronis and Jiři Žák for their constructive reviews. David Pyle is thanked for helpful suggestions. Rakesh Kumar is thanked for sample preparation and magnetic measurements. A research grant from the Department of Science & Technology, Government of India, is gratefully acknowledged.

References

ARANGUREN, A., CUEVAS, J. & TUBIA, J. M. 1996. Composite magnetic fabrics from S–C mylonites. *Journal of Structural Geology* **18**, 863–9.

ARANGUREN, A., TUBIA, J. M., BOUCHEZ, J. L. & VIGNERESSE, J. L. 1996. The Guitiriz Granite, Variscan belt of northern Spain: extension-controlled emplacement of magma during tectonic escape. *Earth and Planetary Science Letters* **139**, 165–76.

BHAT, M. I. 1987. Spasmodic rift reactivation and its role in the pre-orogenic evolution of the Himalayas. *Tectonophysics* **134**, 103–27.

BHAT, M. I., ZAINUDDIN, S. M. & RAIS, A. 1981. Panjal trap chemistry and the birth of Tethys. *Geological Magazine* **118**, 365–75.

BORRADAILE, G. J. & HENRY, B. 1997. Tectonic applications of magnetic susceptibility and its anisotropy. *Earth Science Review* **42**, 49–93.

BOUCHEZ, J. L. 1997. Granite is never isotropic: an introduction to AMS studies of granitic rocks. In *Granite: From Segregation of Melt to Emplacement Fabrics* (eds J. L. Bouchez, D. W. H. Hutton & W. E. Stephens), pp. 95–112. Dordrecht, The Netherlands: Kluwer Academic Publishers.

BOUILLIN, J. P., BOUCHEZ, J. L., LESPINASSE, P. & PECHER, A. 1993. Granite emplacement in an extensional setting: an AMS study of the magmatic structures of Monte Capanne (Elba, Italy). *Earth and Planetary Science Letters* **118**, 263–79.

CASTRO, A. & FERNÁNDEZ, C. 1998. Granite intrusion by externally induced growth and deformation of the magma reservoir: the example of the Plasenzuela pluton, Spain. *Journal of Structural Geology* **20**, 1219–28.

CHATTERJI, G. C. & SWAMINATH, J. 1977. The stratigraphy and structure of parts of the Simla Himalaya – a synthesis. *Memoir of the Geological Survey of India* **106**, 408–88.

CORRY, C. E. 1988. *Laccoliths – mechanics of emplacement and growth*. Geological Society of America, Special Paper no. 220, 120 pp.

DUBEY, A. K., BHAKUNI, S. S. & SELOKAR, A. D. 2004. Structural evolution of the Kangra recess, Himachal Himalaya: a model based on magnetic and petrofabric strains. *Journal of Asian Earth Sciences* **24**, 245–58.

GAETANI, M., GARZANTI, E. & TINTORI, A. 1990. Permo-Carboniferous stratigraphy in SE Zanskar and NW Lahaul (NW Himalaya, India). *Eclogae Geologicae Helvetiae* **83**, 143–61.

GEOFFREY, L., OLIVIER, P. & ROCHETTE, P. 1997. Structure of a hypovolcanic acid complex inferred from magnetic susceptibility anisotropy measurements: the Western Red Hills granites Skye, Scotland, Thulean Igneous Province. *Bulletin of Volcanology* **59**, 147–59.

GURURAJAN, N. S. & VIRDI, N. S. 1984. Superimposition of Early Paleozoic contact metamorphism by Tertiary regional metamorphism around Dalash, district Kulu, Himachal Pradesh (India). *Journal of the Geological Society of India* **25**, 522–7.

HUTTON, D. H. W. & DUMPSTER, T. J., BROWN, P. E. & BECKER, S. D. 1990. A new mechanism of granite emplacement: intrusion in active extensional shear zones. *Nature* **343**, 452–5.

HUTTON, D. H. W. & REAVY, R. J. 1992 Strike-slip tectonics and granite petrogenesis. *Tectonics* **11**, 960–7.

ISLAM, R., UPADHYAY, R., AHMED, T., THAKUR, V. C. & SINHA, A. K. 1999. Pan-African Magmatism, and Sedimentation in the NW Himalaya. *Gondwana Research* **2**, 263–70.

JÄGER, E., BHANDARI, A. K. & BHANOT, V. B. 1971. Rb–Sr age determination of biotites and whole rock samples from the Mandi-Karsog and Chor Granite (H.P.) India. *Eclogae Geologicae Helvetiae* **64**, 523–7.

JELINEK, V. 1981. Characterization of the magnetic fabric of rocks. *Tectonophysics* **79**, T63–7.

LEFORT, P. 1975. Himalaya: the collided range. Present knowledge of the continental arc. *American Journal of Science* **275**, 1–44.

MILLER, C., THÖNI, M., FRANK, W., GRASEMANN, B., KLÖTZLI, U., GUNTLI, P. & DRAGANITS, E. 2001. The early Palaeozoic magmatic event in the northwest Himalaya: source, tectonic setting and age of emplacement. *Geological Magazine* **138**, 237–51.

O'DRISCOLL, B., TROLL, V. R., REAVY, R. J. & TURNER, P. 2006. The Great Eucrite intrusion of Ardnamurchan, Scotland: Reevaluating the ring-dike concept. *Geology* **34**, 189–92.

PATERSON, S. R., FOWLER, T. K., SCHIMDT, K. L., YOSHINOBU, A. S., YUAN, E. S. & MILLER, R. B. 1998. Interpreting magmatic fabric patterns in plutons. *Lithos* **44**, 53–82.

PETRONIS, M. S., O'DRISCOLL, B., TROLL, V. R., EMELEUS, C. H. & GEISSMAN, J. W. 2009. Palaeomagnetic and anisotropy of magnetic susceptibility data bearing on the emplacement of the Western Granite, Isle of Rum, NW Scotland. *Geological Magazine* **146**, 419–36.

PILGRIM, G. E. & WEST, W. D. 1928. *Structure and correlation of Simla Rocks*. Geological Survey of India (Memoirs) no. 53, 139 pp.

ROCHETTE, P. 1987. Magnetic susceptibility of the rock matrix related to magnetic fabric studies. *Journal of Structural Geology* **9**, 1015–20.

SEN, K. & MAMTANI, M. A. 2006. Magnetic fabric, shape preferred orientation and regional strain in granitic rocks. *Journal of Structural Geology* **28**, 1870–82.

SRIKANTIA, S. V. & BHARGAVA, O. N. 1979. The Tandi Group of Lahaul – its geology and relationship with the Central Himalayan Gneiss. *Journal of the Geological Society of India* **29**, 531–9.

SRIKANTIA, S. V. & BHARGAVA, O. N. 1998. *Geology of Himachal Pradesh*. Geological Society of India (Bangalore), 408 pp.

STECK, A. 2003. Geology of the NW Indian Himalaya. *Eclogae Geologicae Helvetiae* **96**, 147–96.

STEVENSON, C. T. E., OWENS, W. H. & HUTTON, D. W. H. 2007. Flow lobes in granite: the determination of magma flow direction in the Trawenagh Bay Granite, N. W. Ireland, using anisotropy of magnetic susceptibility. *Geological Society of America Bulletin* **119**, 1368–86.

TARLING, D. H. & HROUDA, F. 1993. *The Magnetic Anisotropy of Rocks*. London: Chapman & Hall, 212 pp.

THAKUR, V. C. 1975. Some genetic significance of the development of foliation and lineation in the Dalhousie Granite body and surrounding metasedimentary formations of Chamba area of Himachal Pradesh. In *Recent Researches in Geology, vol. 2* (ed. P. K. Verma *et al.*), pp. 41–52. Delhi: Hindustan Publishing Corporation.

THAKUR, V. C. & RAWAT, B. S. 1992. *Geological Map of the Western Himalaya. Scale 1:1,111,111*. Dehra Dun: Wadia Institute of Himalayan Geology.

TOMEZOLLI, R. N., MCDONALD, W. D. & TICKYJ, H. 2003. Composite magnetic fabrics and S–C structures

in granite gneiss of Cerro de los Viejos, La Pampa province, Argentina. *Journal of Structural Geology* **5**, 351–68.

VALDIYA, K. S. 1993. Evidence for Pan African–Cadomian tectonic upheavals in Himalaya. *Journal of the Palaeontological Society of India* **38**, 51–62.

VALDIYA, K. S. 1995. Proterozoic sedimentation and Pan-African geodynamic development in the Himalaya. *Precambrian Research* **74**, 35–55.

VIRDI, N. S. 1994. Basement structures and their possible relation to sedimentation and tectonics in the Tethyan Basin of Western Himalaya. *Journal of Himalayan Geology* **5**, 11–19.

https://doi.org/10.1017/S0016756810000105 Published online by Cambridge University Press